Orbit Interpolation from Optical Observations

Aymeric Labarbe, Anna Schwab, Philippe Gigon
EPFL

May 30, 2022

Abstract

In this paper, different ways of preliminary orbit determination from optical sightings with a telescope, are implemented and tested. Starting from long exposure images taken with a Celestron RASA 36 telescope, the aim is to detect satellites and satellite debris on the image, extract their position and interpolate a first estimate of the object's orbit. The orbit determination is done with two different preliminary orbit determination algorithms, namely a Laplace and a Gaussian algorithm. The two algorithms are tested in various cases and with data provided by Stellarium. In the tested cases the two algorithms lead to similar results. In most of the tested cases the obtained heights are up to few percent of relative error close to the real orbits. Nevertheless, in some situations the preliminary orbit determination fails and large errors on the satellite's height and velocity occur. It was not possible to uniquely identify the reasons for those failures, different studied parameters such as the elevation of the observed satellite and the time between two observations have been identified as critical parameters. Tests with real data have been done and give more imprecise results. It could be due to the difficulty of extracting the angles from the images. In fact, further algorithmic work is needed in order to improve those results.

Contents

1 Introduction

The low Earth orbit (LEO) was host to the very first satellite ever launched, Sputnik 1 [1] in 1958. From then, the number of satellites populating the orbits between 160 km to 1000 km above Earth [2] has steadily increased. Today, more than 3400 active satellites are found in these orbits as well as more than 5000 non-functional objects, like space-debris [3]. The EPFL association Space Situational Awareness Team has the goal of tracking these satellites and debris using a telescope in order to get a better idea of the actual population of the low Earth orbit, as well as the potential dangers that come with an increasing population. This project aims at predicting the orbit of an observed object using the association's telescope. The telescope is connected to a camera, which takes the pictures used for the tracking. These pictures contain tracks of the satellites, due to the long exposure time and reflected sunlight. From the tracks, coordinates are extracted and are then used to calculate the satellite's orbit. The orbit calculations are done in two major steps: The first one is the Gauss (or Laplace) algorithm, which finds iteratively the preliminary orbit, consisting of the vector from the Earth's center to the satellite as well as its velocity. The second step is the calculation of the orbital elements which define the orbit uniquely, and the formatting of the elements in a predefined output format, the two line element TLE. This is the most common format used to display and store information of an object in orbit.

In this paper the algorithms used to compute the position and velocity of the object and to find the orbital elements are explained. Furthermore, the data acquisition procedure is described. Finally, data provided by different institutions, such as NORAD, is used to check the validity of the obtained results. The impacts of different parameters, such as the time between the observations and the elevation angle of the satellite, are studied.

2 Theory

2.1 IOD and TLE format

The input and output formats of the algorithm consist of two distinct, well defined and widely used data sets.

2.1.1 IOD

```
00000 03 123XYZ 0000 G YYYYMMDDHHMMSSsss 00 45 DDDMMSSs+DDMMSSs 00 B+MMm Mm SSSsss
```

Figure 1: IOD format with extended precision.

The input of the algorithm is given by the IOD (Interactive Orbit Determination) format. This format contains the exact time of the observation, the measured angles and other information allowing to determine the observers location. The angles can be given in different formats, figure 1 shows the format corresponding to Degree-Minute-Second (DMS). In order to find the orbits, three IODs are needed as well as the position of the observer.

2.1.2 TLE

A satellite's orbit can be described at a certain time using the Two Line Element set TLE (see figure 2). The format, originally used mostly by the United States military and NASA, has become the most common data format for the localization of satellites. As the name says, the TLE consists of two lines of data, where information of the satellite is stored. Some of this information concerns the administration of the satellite such as its catalogue number, its international designator[1], its classification and several more. For this project, these entries do not matter and are therefore set to 0. The other values define the satellites orbit and its position at the time, when the observation was made.

[1] last two digits of launch year, launch number of the year, piece of the launch [4].

```
1 00000U 00000000 22117.44211806 0.0000000 0000000000 00000000 0 00000
2 00000 097.2225 168.7478 0016232  84.9179 337.6234 15.367583120000000
```

Figure 2: TLE format.

In figure 2, an example of a TLE is shown. Both of the lines are headed by their relative line number and the satellite catalogue number consisting of 5 figures, set to "00000" in this example. In the first line, the only non-zero value is the epoch time (the time of observation), where the first two figures ("22" in figure 2) correspond to the last two digits of the year when the observation was done. The following three digits with the decimals is the day and the time in the unit of days. The second line of the TLE contains, after the line number and the satellite catalogue number, the orbital elements of the satellite's orbit at the time of observation. The orbital elements are (from left to right) the inclination, the right ascension of the ascending node, the decimal places of the eccentricity, the argument of perigee, the mean anomaly, and the mean motion. A detailed explanation and the calculation of these values will be done later in section 3.4.

2.2 Coordinate systems

In order to calculate the orbits, the angles of the satellites are provided through the IOD. The IOD format supports two celestial coordinate systems: the horizontal and the equatorial coordinate systems.

Horizontal coordinates The horizontal coordinate system is a local coordinate system, that depends on the position of the observer. In this system the observer's horizon defines a plane, and the first angle, the altitude a (or elevation), corresponds to the angle between the observed object and the plane. The second angle, the azimuth A, is defined as the angle between the projection of the object on the horizontal plane, and the north pole. Thus, due to the Earth's rotation, the angle of a geostationary object will not change with time.

Equatorial coordinates The equatorial coordinate system is a non-local coordinate system, defined by an origin at the center of the Earth. Such a system is called geocentric while a system defined on the Earth's surface is called topocentric. In this system, the equatorial plane (the reference plane), corresponds to the projection of the equator on the celestial sphere. On the celestial equator, the intersection of the equatorial and ecliptic[2] planes define two fixed points, one of them is called the 'vernal point'. The first angle, the right ascension α, corresponds to the angle of the projection of the object position on the equatorial plane, positive eastward from the the vernal point. The declination δ, the second angle, measures the angle perpendicular to the equatorial plane, positive northward from the vernal point. Nonetheless, due to to the precession of the axis of the Earth, the vernal point moves slowly and it has been decided to keep the position of the vernal point of the 1 January 2000 as the reference of the equatorial coordinates. The advantage of this system is, that the coordinates are the same for all observers and that the coordinates of background stars remain the same.

The equatorial coordinate system is sometimes generalized for an observer on the Earth's surface by just translating the origin and the associate reference frame to the observer. The angles in this frame correspond to the geocentric equatorial angles of the background which differs from the geocentric equatorial angles of the observed object if this object is not infinitely far away. The two system of coordinates are illustrated on figure 3.

[2]The ecliptic plane correspond to the plane defined by the orbit of the Earth around the sun.

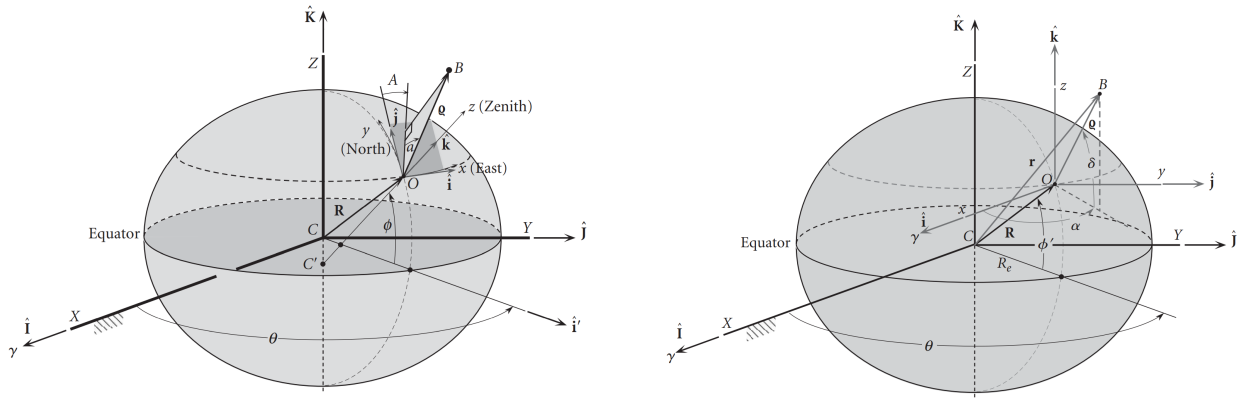

(a) (b)

Figure 3: Topocentric a) horizontal coordinates and b) equatorial coordinates [5].

3 Algorithms

Preliminary orbit determination is a category of procedures to get a first estimate of the orbit without considering perturbations such as atmospheric drag, gravitational effects from the sun and the moon and others. There are two different situations:

- If one has access to distance measurements (range), the orbit can be determined with two position vectors and the corresponding observational times. The problem is reduced to the mathematical problem of ellipsis interpolation (Gibb's method).
- If one only has access to angle measurement, three sets of two angles and the observational times are needed to give an approximate orbit.

Since range measurements are inaccessible with the given setup, the second method is needed. The Gaussian and Laplacian preliminary orbit determination algorithms have been implemented.

3.1 Basis vectors

The starting point of all the implemented algorithms is to define the unit vectors that point from the observer to the satellite and the vectors that indicate the observer's position with respect to the center of Earth in the same basis. The chosen basis is the vector basis $(\hat{\mathbf{I}}, \hat{\mathbf{J}}, \hat{\mathbf{K}})$ associated to the equatorial system (which is the same for the geocentric and topocentric equatorial system) as illustrated in figure 3. For an observer at geodetic latitude ϕ, altitude H at time t the vector position $\hat{\mathbf{R}}$ is given by :

$$\mathbf{R} = \Big(\frac{R_e}{\sqrt{1-(2f-f^2)\sin^2(\phi)}}+H\Big)\cos(\phi)\Big(\cos(\theta(t))\hat{\mathbf{I}}+\sin(\theta(t))\hat{\mathbf{J}}\Big)+\Big(\frac{R_e(1-f)^2}{\sqrt{1-(2f-f^2)\sin^2(\phi)}}+H\Big)\sin(\phi)\hat{\mathbf{K}},$$

where $f = \Big(\frac{R_e - R_p}{R_e}\Big) = 3.33\times10^{-3}$ is the oblateness of the Earth [6] and R_e, R_p, respectively the equatorial and polar radius of the Earth. $\theta(t)$ is the local sidereal time of the observer which corresponds to the angle between the observer and the vernal point.
For topocentric equatorial angles, the unit vectors are defined as in equation (1):

$$\boldsymbol{\rho_i} = \cos(\delta_i)\cos(\alpha_i)\hat{\mathbf{I}} + \cos(\delta_i)\sin(\alpha_i)\hat{\mathbf{J}} + \sin(\delta_i)\hat{\mathbf{K}}. \tag{1}$$

Since horizontals angles are also used, the unit vectors were also implemented for this coordinate system:

$$\boldsymbol{\rho_i} = \begin{pmatrix} -\sin(\theta(t_i)) & -\sin(\phi_i)\cos(\theta(t_i)) & \cos(\phi_i)\cos(\theta(t_i)) \\ \cos(\theta(t_i)) & -\sin(\phi_i)\sin(\theta(t_i)) & \cos(\phi_i)\sin(\theta(t_i)) \\ 0 & \cos(\phi_i) & \sin(\phi_i) \end{pmatrix} \begin{pmatrix} \cos(a_i)\sin(A_i) \\ \cos(a_i)\cos(A_i) \\ \sin(a_i) \end{pmatrix}. \tag{2}$$

To summarize, the needed input data is the altitude, latitude and longitude (to calculate the sidereal time) of the observers, the angles of the observed object in horizontal or topocentric equatorial coordinates, and the time of observation in the UTC format.

3.2 Gauss algorithm

The initial data are the unit vectors $\boldsymbol{\rho}_i$ pointing from the observer towards the satellite, the corresponding times t_i and the positions of the telescope $\mathbf{R}_i$ (usually the telescope is stationary, hence the $\mathbf{R}_i$ are all the same). The position of the satellite can thus be expressed in the following way:

$$\mathbf{r}_i = \mathbf{R}_i + \rho_i \boldsymbol{\rho}_i, \tag{3}$$

as illustrated in figure 4 and with ρ_i the unknown distance from observer to satellite. It is furthermore known that the three vectors must lie in the same plane (by conservation of angular momentum) giving the additional relation:

$$\mathbf{r}_2 = c_1 \mathbf{r}_1 + c_3 \mathbf{r}_3. \tag{4}$$

Finally, the positions at time t_1, t_3 can be expressed by the position at time t_2 using the Lagrange coefficients f_i, g_i:

$$\begin{aligned} \mathbf{r}_1 &= f_1 \mathbf{r}_2 + g_1 \mathbf{v}_2, \\ \mathbf{r}_3 &= f_3 \mathbf{r}_2 + g_3 \mathbf{v}_2. \end{aligned} \tag{5}$$

For sufficiently short time intervals between the observations, the Lagrange coefficients can be approximated and depend only on r_2 and the corresponding times. With this, the problem is reduced to a system of equations which can be solved approximately.

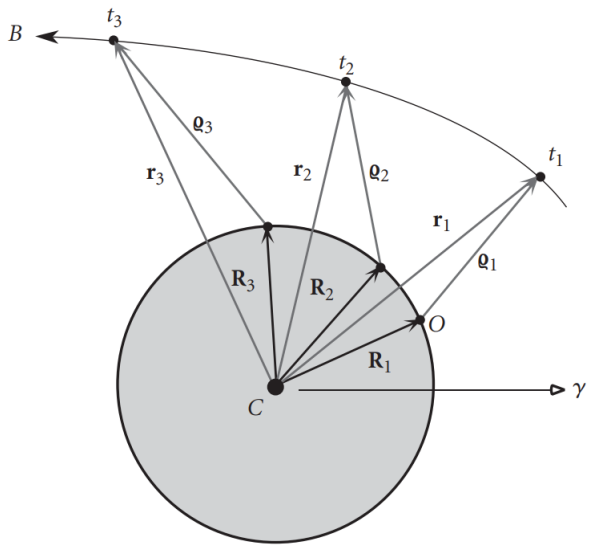

Figure 4: Gauss method: Finding the position vectors $\mathbf{r}_i$ from the position of the observer $\mathbf{R}_i$ and the observed position vectors $\boldsymbol{\rho}_i$ [5].

Starting from equation (4), one can isolate the two coefficients c_1, c_2 by taking the cross product on both sides of the equation:

$$\begin{aligned} c_1 &= \frac{(\mathbf{r}_2 \times \mathbf{r}_3) \cdot (\mathbf{r}_1 \times \mathbf{r}_3)}{|\mathbf{r}_1 \times \mathbf{r}_3|^2}, \\ c_3 &= \frac{(\mathbf{r}_2 \times \mathbf{r}_1) \cdot (\mathbf{r}_3 \times \mathbf{r}_1)}{|\mathbf{r}_1 \times \mathbf{r}_3|^2}. \end{aligned} \tag{6}$$

Using the Lagrange coefficients (equation (5)) the coefficients c_1, c_3 can be expressed as follows:

$$\begin{aligned} c_1 &= \frac{g_3}{f_1 g_3 - f_3 g_1}, \\ c_3 &= -\frac{g_1}{f_1 g_3 - f_3 g_1}. \end{aligned} \tag{7}$$

Up to this point, all the equations are exact and have been derived using Kepler's equations of motion and simple vector algebra. Here, one needs to do a first approximation in order to find the Lagrange coefficients. To do so, the coefficients are approximated as:

$$\begin{aligned} f_i &\approx 1 - \frac{\mu}{2r_2^3}(\Delta t_i)^2, \\ g_i &\approx \Delta t_i - \frac{\mu}{6r_2^3}(\Delta t_i)^3, \end{aligned} \tag{8}$$

with $\Delta t_i = t_i - t_2$ and $\mu = GM_E = 3.986004418 \times 10^{14} \mathrm{m^3 s^{-2}}$ Earth's standard gravitational parameter [7]. Using those expressions and further Taylor expanding them, one can find the following approximate values for the coefficients c_1, c_2:

$$\begin{aligned} c_1 &\approx \frac{\Delta t_3}{\Delta t}\left[1 + \frac{1}{6}\frac{\mu}{r_2^3}\left(\Delta t^2 - \Delta t_3^2\right)\right], \\ c_3 &\approx -\frac{\Delta t_1}{\Delta t}\left[1 + \frac{1}{6}\frac{\mu}{r_2^3}\left(\Delta t^2 - \Delta t_1^2\right)\right], \end{aligned} \tag{9}$$

with $\Delta t = t_3 - t_1$. Using those values in equation (4) and the definition of $\mathbf{r}_i = \mathbf{R}_i + \rho_i \boldsymbol{\rho}_i$ one can find approximations for the different distances ρ_i and finally the desired $\mathbf{r}_2$. Using again equation (5) one can solve for $\mathbf{v}_2$ and find:

$$\mathbf{v}_2 = \frac{f_1 \mathbf{r}_3 - f_3 \mathbf{r}_1}{f_1 g_3 - f_3 g_1}. \tag{10}$$

This gives a first estimate for $\mathbf{r}_2, \mathbf{v}_2$. This values are then used to iteratively find better results by solving the universal Keppler equation. For details see [5].

3.3 Laplace algorithm

As an alternative to Gauss's algorithm, a version of the Laplace algorithm was also implemented, based on Bate, Mueller and White: Fundamentals of Astrodynamics [8]. This algorithm has the goal of calculating the position and the velocity of the observed satellite based on three observation points. The input is again the three sets of topocentric angles. A first difference to Gauss's algorithm is already here: while Gauss's algorithm needs strictly three IODs, Laplace's algorithm has no upper limit of observations. However, for this project, the version that takes three input observations is used. For three inputs, the Laplace algorithm will return the position and the velocity at the center observation, at time t_2.

As in the Gauss algorithm, the starting point is equation (3). This equation is then differentiated twice and one finds

$$\ddot{\boldsymbol{r}}_{\boldsymbol{i}} = 2\dot{\rho}_i \dot{\boldsymbol{\rho}}_{\boldsymbol{i}} + \ddot{\rho}_i \boldsymbol{\rho}_i + \rho_i \ddot{\boldsymbol{\rho}}_i + \ddot{\boldsymbol{R}}. \tag{11}$$

In addition, the equation of motion gives

$$\ddot{\boldsymbol{r}}_i = -\mu \frac{\boldsymbol{r}}{r^3}. \tag{12}$$

The two observed angles are used to define the unit vectors $\boldsymbol{\rho_i}$ pointing from the observer to the object. The unit vector is given at three different times, which enables the numerical differentiation of the unit vector at the central time and one can obtain $\dot{\boldsymbol{\rho}}_{\boldsymbol{2}}$ and $\ddot{\boldsymbol{\rho}}_{\boldsymbol{2}}$. The Lagrange interpolation formula is then used to write a general expression for the unit vector $\boldsymbol{\rho}$ as a function of time:

$$\boldsymbol{\rho(t)} = \frac{(t-t_2)(t-t_3)}{(t_1-t_2)(t_1-t_3)}\boldsymbol{\rho_1} + \frac{(t-t_1)(t-t_2)}{(t_2-t_1)(t_2-t_3)}\boldsymbol{\rho_2} + \frac{(t-t_1)(t-t_2)}{(t_3-t_1)(t_3-t_2)}\boldsymbol{\rho_3}. \tag{13}$$

For more than three observations, the unit vector $\boldsymbol{\rho}(t)$ is interpolated using all the observations and therefore, a more accurate value of $\boldsymbol{\rho}(t)$ can be found. $\boldsymbol{\rho}(t)$ can be differentiated and one finds $\dot{\boldsymbol{\rho}}(t)$ and $\ddot{\boldsymbol{\rho}}(t)$:

$$\dot{\boldsymbol{\rho}}(t) = \frac{2t - t_2 - t_3}{(t_1 - t_2)(t_1 - t_3)}\boldsymbol{\rho_1} + \frac{2t - t_1 - t_3}{(t_2 - t_1)(t_2 - t_3)}\boldsymbol{\rho_2} + \frac{2t - t_1 - t_2}{(t_3 - t_1)(t_3 - t_2)}\boldsymbol{\rho_3}, \tag{14}$$

$$\ddot{\boldsymbol{\rho}}(t) = \frac{2}{(t_1 - t_2)(t_1 - t_3)}\boldsymbol{\rho_1} + \frac{2}{(t_2 - t_1)(t_2 - t_3)}\boldsymbol{\rho_2} + \frac{2}{(t_3 - t_1)(t_3 - t_2)}\boldsymbol{\rho_3}. \tag{15}$$

The numerical values for the central time can be found by setting $t = t_2$ in equation (14), which can then be inserted in the combined equations (11) and (12) with $i = 2$. One can find a system of three equations with four unknowns: $r_2, \rho_2, \dot{\rho}_2$ and $\ddot{\rho}_2$. The system is solved for ρ_2 as a function of r_2. Equation (3) is dotted with itself:

$$r_2^2 = \rho_2^2 + 2\rho_2\boldsymbol{\rho}_2 \cdot \boldsymbol{R} + \boldsymbol{R}^2. \tag{16}$$

Inserting the previously found solution of ρ_2 in equation (16) gives an eighth order equation that one can solve iteratively for $\boldsymbol{r}_2$. Applying the same procedure with $\dot{r}_2$ and $\dot{\rho}_2$, one finds the velocity $\boldsymbol{v}_2$.

3.4 Computation of the orbital elements

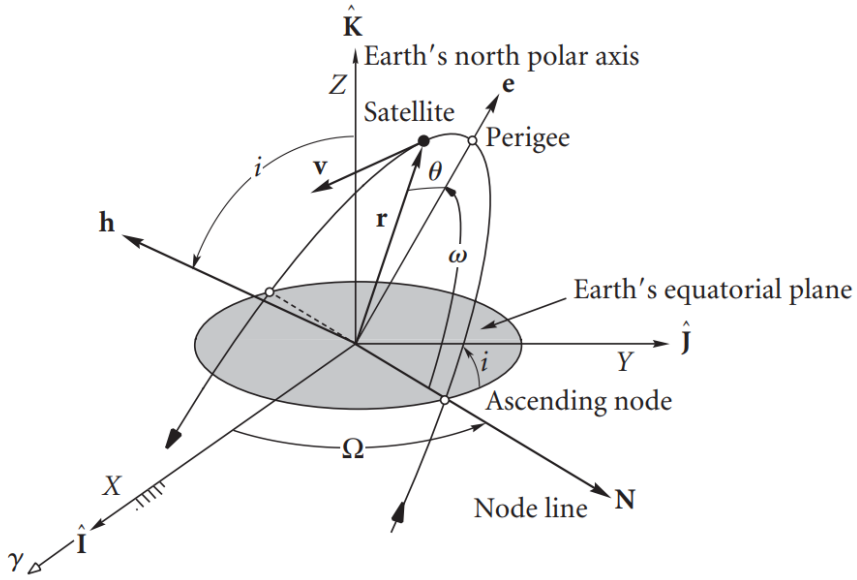

Figure 5: The orbital elements that define the trajectory of a satellite [5].

The orbital elements defining the satellite's path and therefore used for a TLE are depicted in figure 5. They are calculated using a formalism that takes the position $\mathbf{r}$ and the velocity $\mathbf{v}$ at the chosen epoch time. In the following calculations u_i indicates the i-component of the vector $\boldsymbol{u}$.
First, some auxiliary values are calculated that are needed for the determination of the elements. The norm of the radial velocity v_r is given by:

$$v_r = \frac{\mathbf{r} \cdot \mathbf{v}}{r}. \tag{17}$$

The specific angular momentum $\mathbf{h}$:

$$\mathbf{h} = \mathbf{r} \times \mathbf{v} \qquad \Rightarrow \qquad h = \sqrt{\mathbf{h} \cdot \mathbf{h}}. \tag{18}$$

From the specific angular momentum, one can calculate the first orbital element, the inclination i:

$$i = \cos^{-1}\left(\frac{h_z}{h}\right). \tag{19}$$

The node line $\mathbf{N}$ is another auxiliary value:

$$\mathbf{N} = \hat{\mathbf{K}} \times \mathbf{h} \qquad \Rightarrow \qquad N = \sqrt{\mathbf{N} \cdot \mathbf{N}}. \tag{20}$$

Using the node line N, one finds the right ascension of the ascending node Ω. The y-component of the node line indicates, whether Ω is placed in the correct quadrant. Therefore, one has:

$$\Omega = \begin{cases} \cos^{-1}\left(\frac{N_x}{N}\right) & \text{if} \quad N_y \geq 0 \\ 360^\circ - \cos^{-1}\left(\frac{N_x}{N}\right) & \text{if} \quad N_y < 0 \end{cases} \tag{21}$$

The next orbital element calculated is the eccentricity:

$$\mathbf{e} = \frac{1}{\mu}\left[\mathbf{v} \times \mathbf{h} - \mu\frac{\mathbf{r}}{r}\right] \qquad \Rightarrow \qquad e = \sqrt{\mathbf{e} \cdot \mathbf{e}}, \tag{22}$$

where μ is the standard gravitational parameter of the Earth as defined previously. With the eccentricity $\mathbf{e}$ and the node line $\mathbf{N}$, it is possible to find the argument of perigee. Similar to the right ascension of the ascending node, one has to test whether the value is placed in the correct quadrant, for which the z-component of the eccentricity has to be considered:

$$\omega = \begin{cases} \cos^{-1}\left(\frac{\mathbf{N}\cdot\mathbf{e}}{Ne}\right) & \text{if} \quad e_z \geq 0 \\ 360^\circ - \cos^{-1}\left(\frac{\mathbf{N}\cdot\mathbf{e}}{Ne}\right) & \text{if} \quad e_z < 0 \end{cases} \tag{23}$$

In order to find the mean anomaly M, one has to determine first the true anomaly θ. The quadrant of the true anomaly is determined by the sign of the radial velocity v_r:

$$\theta = \begin{cases} \cos^{-1}\left(\frac{\mathbf{e}\cdot\mathbf{r}}{er}\right) & \text{if} \quad v_r \geq 0 \\ 360^\circ - \cos^{-1}\left(\frac{\mathbf{e}\cdot\mathbf{r}}{er}\right) & \text{if} \quad v_r < 0 \end{cases} \tag{24}$$

From the true anomaly, one can compute the mean anomaly M, using the eccentric anomaly E [9]. The mean anomaly M is an orbital element used for the TLE:

$$E = \sin^{-1}\left(\frac{\sin\theta\sqrt{1-e^2}}{1+e\cos\theta}\right) \qquad \Rightarrow \qquad M = E - e\sin E. \tag{25}$$

The last orbital element that is computed for the TLE is the mean motion n, meaning the number of revolutions around Earth completed by the satellite in a day. To do so, one first needs the semi-major axis u, calculated with the two equations that define the semi-parameter p [9]:

$$p = \frac{h^2}{\mu} \qquad \text{and} \qquad p = u(1-e^2) \quad \Rightarrow \quad u = \frac{h^2}{\mu(1-e^2)} \tag{26}$$

$$\Rightarrow \qquad n = \sqrt{\frac{\mu}{u^3}}. \tag{27}$$

4 Experimental Setup

The experimental setup consists in a Celestron RASA (Rowe-Ackermann Schmidt Astrograph) 36 telescope (see figure 6b) and an astrophotography camera (see figure 6a). The telescope is installed on an equatorial mount allowing to compensate the rotation of Earth. The telescope having a focal length of 790 mm and a focal ratio of f/2.2, is ideally fitted for the observation of satellites. In order to detect satellite tracks, the telescope captures the sunlight reflected by the satellites and due to the high velocity of the satellite in comparison to the exposure time, the satellite's trace appears. This imposes an important constraint on the experiment: The satellites are only illuminated for a few hours after sunset. It is furthermore important to have as little light pollution as possible. The ideal site for observations is the Astroval observatory in the Vallée de Joux, nevertheless many measurements have also been taken on the roof of the Cubotron building at EPFL in order to facilitate the transportation of the telescope. A further restriction is the weather: The sky has to be completely cloudless in order to take valid and usable measurements.

(a)

(b)

Figure 6: a) ZWO Mono astrocamera used for observations b) Telescope and mount image by Yan Crevoisier.

4.1 Setting up the telescope

As described above, the telescope is installed on an equatorial mount and it must therefore be aligned with Polaris. The first step is to set up the mount and align it with Earth's axis of rotation. This can be done few minutes after sunset as Polaris is one of the brightest stars in the sky and therefore one of the first that can be seen by eye. The alignment must be done very carefully since it is very difficult to change the alignment of the mount once the heavy telescope is installed on top of it. It can take up to 20 minutes. Once aligned with the rotation axis, the telescope needs to be put in place. As the whole setup weights approximately 100 kg, two to three persons are needed to set everything up. When the telescope is in place, the mount needs to be calibrated. This step is important, as precise knowledge of the telescopes orientation is of great importance. The alignment is done in the following way:

1. Use the GoTo[3] function to point the telescope to a given star.
2. Use the camera and perfectly align the telescope with the given star, therefore correct the errors done by the telescope. Tell the mount the new position.
3. Repeat steps 1 and 2 until the mount perfectly finds the corresponding stars and no correction is needed anymore.

[3]GoTo is a functionality of the mount which allows to move the mount to a specific object in the sky. The telescope uses its azimuth and elevation in order to know its field of view, hence those angles must be calibrated at each use.

To optimize the calibration of the telescope, the chosen stars should not be close to each other. This is one of the reasons, why it is important for the sky to be entirely cloudless. Otherwise, the calibration process is limited to a certain direction range, with a risk of an imprecise calibration.

4.2 Data acquisition

Once the telescope and the mount are installed and calibrated, the data acquisition begins. To do so, the camera is cooled down to -10° C in order to minimize thermal noise on the sensor. Once this temperature is reached, the camera is set up to take long exposure images with exposure times of 0.5 - 2 s. Each image is stored in the FITS (Flexible Image Transport System) format and contains all the relevant information such as exposure time and time at which the image was taken. In principle, the telescope can be oriented to a fixed point in the sky and take images for hours, nevertheless in practice it is more efficient to search for satellites (for example with the application Stellarium) in order to get as many observations with visible satellites as possible.

4.3 Image treatment

The treatment of the images of satellites was subject of two previous projects done for SSA EPFL[4] and it is not a main part of this project. However, the goal being the combination of the two algorithms in order to have an image as an input file and the TLE as an output file did come with some work on these previously done codes.

The idea of the image treatment is to have three consecutive images, with traces of satellites in them, as an input. The algorithm should then find the traces, verify whether they belong to the same satellite and if so, take the middle points of three consecutive traces and give the IODs of these three points as an output. In order to make this algorithm work with the images that were taken by the telescope, different changes had to be done. A first problem that appeared with the images taken by the telescope, were the usually missing consecutive images. As the telescope does not allow active tracking of the satellites, it is difficult to take several images of the same object. Therefore, the algorithm should be altered so it takes only one image with a trace and then returns the beginning, the middle and the end point as IODs each. That way, one still gets the three consecutive IODs needed for the orbit calculation, but only needs one image as an input. The testing of the altered algorithm lead to other changes that have to be done: In comparison to the images, for which the original code was written, the telescope's pictures have much more background noise. This is mostly due to the short exposure time of $0.5 - 2$ s. The filter that is used in the code to reinforce the light pixels of the trace also reinforces all of the noise and the picture becomes unreadable for the algorithm. Hence, another filter was created, deleting the background noise, as well as some of the small stars due to the filter's nature of only keeping accumulations of more than 100 bright pixels. This process is shown in figure 7. Figure 7a shows an unfiltered image taken with the telescope of the Starlink satellite SL-1186. The treated image is shown on the right side, in figure 7b. One can see, that the background noise was deleted successfully, however, one also remarks that the satellite's trace has become thicker. After several tests, it has become clear, that this trace is too thick for the algorithm to detect and therefore, that it is not possible to use the simple noise filter as it is implemented. Due to the complexity of the problem and the fact that this is not a major part of the project, there was no further work done on this matter. Another reason is, that this problem is currently treated by a master student for the association.

4.4 Extracting the angles

Once the satellite track is detected on the image, the coordinates of the satellite have to be extracted. This can be done using plate solving: By comparison of the stars in the picture with a reference catalogue, a specialized program can give the equatorial coordinates of the track. As the line was not available for the reasons described above, the extraction of the coordinates was done manually. This procedure is very imprecise as the tracks have a considerable thickness and hence the extracted angles come with a large uncertainty, in fact the tracks have angular widths of $(11 \pm 1)''$. As precise angle measurements are essential

[4]Yann Bouquet: *Delineating Satellite Tracks in Astronomical Images*, Manon Béchaz, Baptiste Claudon, Jules Eschbach and Salomon Guinchard: *Detecting orbital objects with optical camera.*

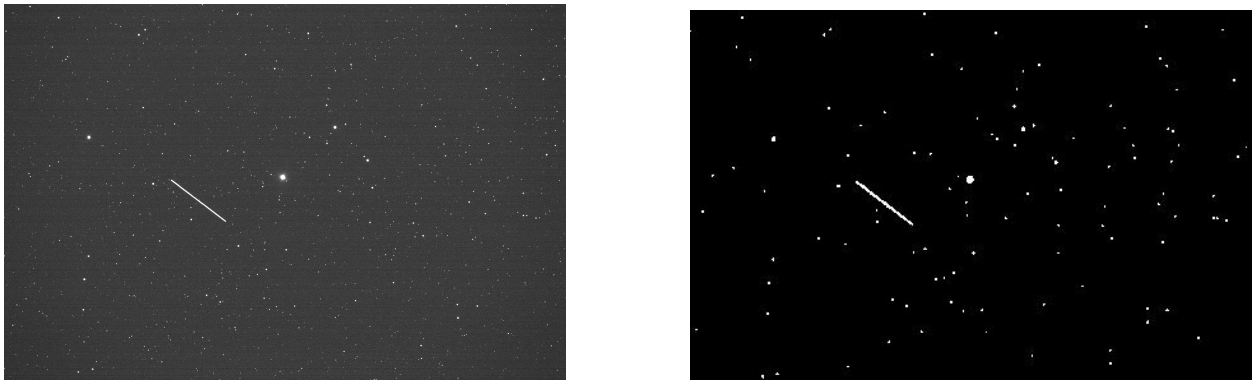

(a) (b)

Figure 7: a) Unfiltered and b) filtered image.

for correct functioning of the preliminary orbit determination, the orbits obtained with those data input are very far from the actual orbits (choosing one side of the track rather than the center gave relative errors up to 100 % on the satellites height!). For those reasons the tests of the algorithm have mostly been done with data provided on the internet.

5 Testing the Algorithms

5.1 Gauss algorithm

In order to test the algorithm, precise data was needed. As the extraction of the coordinates from the images was not possible, the tests have been done with satellite positions obtained from Stellarium and OrbTrack [10, 11]. Those websites provide the topocentric azimuth and elevation of celestial objects predicted using the orbital elements of the corresponding object. The obtained results have been compared to TLEs provided by different institutions such as NORAD and NASA [12].

Table 1 shows different orbital elements computed with the implemented Gauss algorithm. The table contains, in the same order: the name of the satellites, the time difference between the observations, the altitude r of the satellite, its speed and the mean motion (revolutions per day) with the corresponding relative differences, the orbital elements inclination i, the right ascension of the ascending node Ω, the eccentricity e and the relative errors on those quantities. In the case of Calipso, no reference speed was available. Starlink-1046 is an example of a failure of the algorithm: the eccentricity is larger than one, indicating that the orbit is not closed. On the other hand, the tests done for Nusat-7 with time difference of 60 ± 0.5 s, show results close to the reference values. The relative errors are smaller than 1% for all the quantities except for the eccentricity. Yet, in comparison to the other satellites, even the error on the eccentricity is smaller. All the tests in this table have been done with seven and six digit precision on the angles (corresponding to the maximal precision of the classical IOD format).

		Orbitals parameters			Relatives errors		
Satellite	Δt [s]	r [km]	v [km/s]	n [rpd]	$\Delta r/r$	$\Delta v/v$	$\Delta n/n$
Nusat-7	20.0 ± 0.5	509.05	7.968	13.04	7.2×10^{-2}	4.5×10^{-2}	1.5×10^{-1}
Nusat-7	60.0 ± 0.5	484.39	7.653	15.18	4.2×10^{-3}	3.6×10^{-3}	1.0×10^{-2}
Starlink-2687	15.0 ± 0.5	555.24	7.651	14.70	5.7×10^{-3}	7.7×10^{-3}	2.4×10^{-2}
Calipso	7.0 ± 0.5	702.03	7.774	13.06	1.5×10^{-2}	-	1.2×10^{-1}
Starlink-1046	1.0 ±0.1	725.36	13.38	-	3.1×10^{-1}	7.6×10^{-1}	-
Lemur-2 Tom	6.0 ± 0.5	449.62	7.675	15.25	3.6×10^{-3}	-	1.1×10^{-2}

	Orbitals parameters			Relatives errors		
Satellite	i [°]	Ω [°]	e	$\Delta i/i$	$\Delta\Omega/\Omega$	$\Delta e/e$
Nusat-7	97.27	182.7	9.76×10^{-2}	4.7×10^{-4}	3.2×10^{-3}	74.3
Nusat-7	97.20	182.3	6.20×10^{-3}	2.1×10^{-4}	8.9×10^{-4}	3.8
Starlink-2687	53.02	10.49	17.8×10^{-3}	5.8×10^{-4}	1.5×10^{-1}	10.4
Calipso	97.71	85.13	6.20×10^{-3}	6.0×10^{-3}	5.7×10^{-3}	537
Starlink-1046	59.51	57.33	2.06	1.2×10^{-1}	2.2×10^{-1}	1.2×10^{4}
Lemur-2 Tom	51.78	15.34	1.57×10^{-2}	2.6×10^{-3}	5.4×10^{-2}	30.6

Table 1: Computed orbital elements and comparison with reference values [12].

In the following, the IOD format has been readapted in order to add one digit of precision to the angles. Figure 8a shows the relative difference of the satellites height as function of the time between the observations. One can observe that for short times of less than five seconds, the height of the satellite is underestimated whereas for longer observation times the height is slightly overestimated. Figure 8b shows the relative differences of the satellites height as function of its position at the sky. The heights have been measured for the same time intervals between observations ($\Delta t = 5$ s) at different elevations, i.e. low angles correspond to observations close to the horizon whereas values close to 90° correspond to the zenith. One can see that observations close to the horizon give larger errors than observations closer to the zenith.

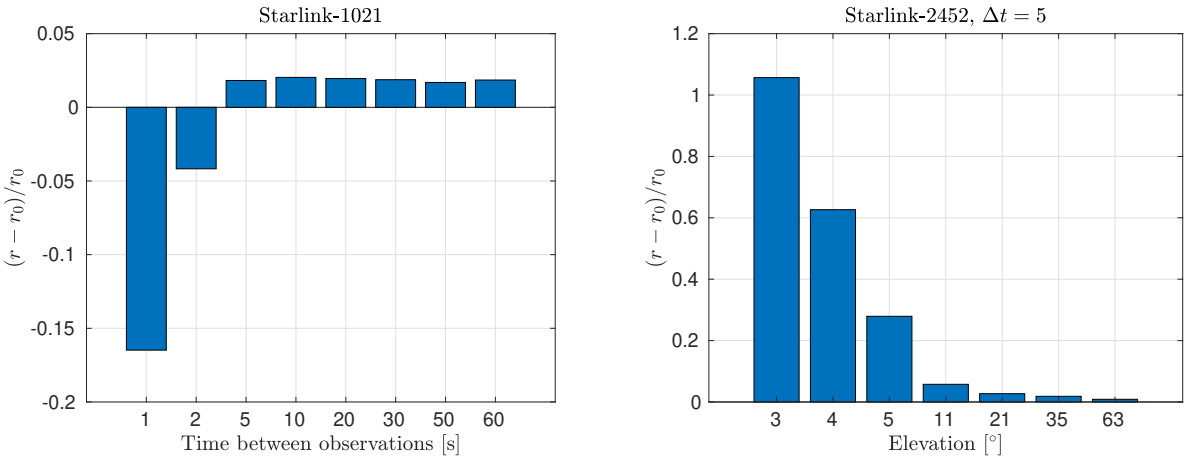

(a) (b)

Figure 8: a) Relative difference of satellite height as function of time between observations b) relative difference of satellite height as function of elevation.

5.2 Laplace and Gauss algorithm comparison

Figure 9 shows the relative errors on the obtained height for the satellites given in table 1 for Gauss and Laplace algorithm. One can see that the results of the two algorithms are always close to each other and sometimes one performs slightly better than the other. One should note that for the satellite which

completely fails, this happens for both of the algorithms. As the two algorithms always give similar results, no further tests have been done for the Laplace algorithm.

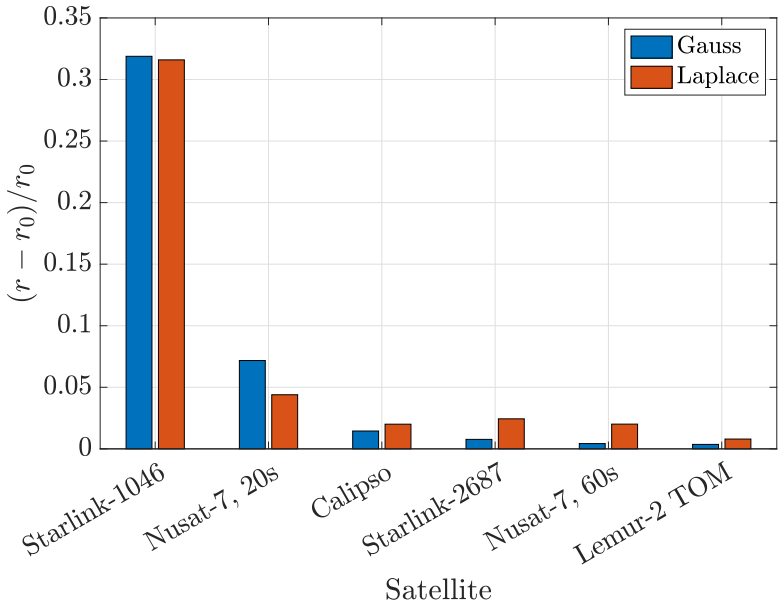

Figure 9: Comparison of the relative differences of Laplace and Gauss algorithm.

5.3 Real image

Figure 10 shows the superposition of three images showing the same satellite. As the telescope points to a fixed part of the sky and the rotation of the Earth is compensated, one can directly superpose three consecutive images as done in this figure. The images have been taken with exposure time of 0.5 s and time between the observations of another 0.5 s, hence the beginning of the first track and the end of the third track are separated by 2.5s. The figure also shows a zoom on the track, where a red dot indicates the chosen position. In fact, the tracks have a considerable width of roughly 10" and therefore it is very difficult to obtain the exact position.

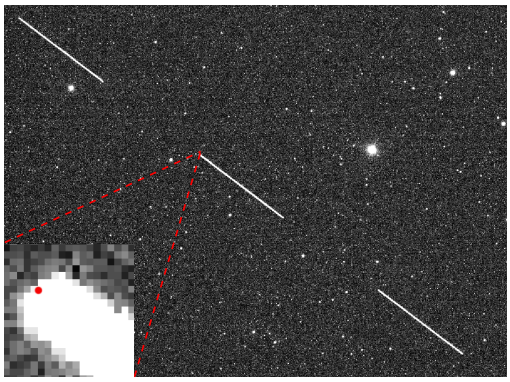

Figure 10: Superposition of three images taken with the telescope, zoom on the track and used position for the orbit interpolation (red dot).

The observation has been done at the Astroval observatory. Using the angles extracted from the images and the corresponding observation times, the algorithm predicts a height of 50 km which is of course absurd.

6 Discussion

As discussed by different authors [13], the Gauss algorithm is sometimes capricious and often gives imprecise orbital elements. This might be due to the fact that the algorithm was initially designed for planets and asteroids which are further from Earth.

Different results obtained with our implementation are shown in table 1. One can see that the relative errors vary strongly from one satellite to the next and also from one orbital element to the next. Comparing the two test done for Nusat-7, once with $\Delta t = 20 \pm 0.5$ s and once with $\Delta t = 60\pm$ s, one can see that the relative errors are significantly smaller for the test with the greater time difference. This leads to a first idea that the time difference might have an important influence on the resulting orbit calculations. This will be further discussed in section 6.1. Once the different relative errors are compared, it is eye-catching that the relative errors of the eccentricity are significantly bigger than the ones for the other orbital elements, whit the smallest error being 380 % for Nusat-7 with a time difference of 60 ± 0.5 s. The great relative errors of the eccentricity will be discussed in section 6.2. Further, this observation supports the hypothesis of the amelioration of the results by using a greater time difference between the observations, as the best result was obtained with the greatest time difference. In contrast to the eccentricity, the inclination of the ellipsis has a comparably low relative errors for all the satellites that are tested. A reason for this might be the fact that it is the first orbital element that is calculated, and therefore, only the errors of the radius and the velocity contribute to the error of the inclination and no further error propagation is included in the value. The two physical quantities directly calculated by the Gauss or the Laplace algorithm are the velocity and the altitude. For the best results in table 1, the relative errors on these two quantities are less than 1%. For example the error on the altitude for the satellite Lemur-2 Tom is 0.36 % which correspond to an error of less than 2 km.

It is in fact very hard to identify the reasons for the differences between the relative errors for the different quantities. The following observations have been made:

- The time difference between the observations is important. In fact, for small Δt the errors are generally larger.
- The different quantities are not all equally concerned by the errors. The inclination, the height and the velocity are rather robust quantities, whereas the eccentricity is very sensitive.
- The elevation of the satellite has an important impact on the predicted orbits.

6.1 Impact of time difference between observations

The first point might be due to the fact that the precision on the angles is limited and always the same. For three points close to each other in time those errors can lead to larger fluctuations as for observations further apart. Figure 8a is giving evidence for this issue. One can also note that for close observations, the algorithm has a tendency to underestimate the height, whereas for longer time intervals the result overestimates the actual height. This is problematic as the time between observations is imposed by the velocity of the satellite and is in practice roughly one second. Due to the properties of the telescope, it is impossible to make the time difference significantly bigger. Furthermore, Gauss algorithm works best for small arcs, i.e. for observations that are very close [14]. This leads to a trade off between smaller and longer times between the observations. Looking at figure 8a, one can also see that for a time difference greater than 5 s between the observations, the errors stays almost constant and is not further lowered. As said before, the Gauss algorithm needs observations that are close together to work properly. This might be the reason for the stagnation of the error.

6.2 Error on the eccentricity

As shown in the table 1, the eccentricity, even in the case of very precise altitude and velocity calculations, is always far form the real value (relative errors of much more than 100%). A sensible question to ask is where this error comes from? In fact, after discussion with experts in the field, it became clear that this is a

known problem of preliminary orbit determination. A set of only few observations (in our case three), leads rarely to precise eccentricities. This can be understood in the following intuitive way: If there are only three approximately known points on the orbit and they are close to each other, each error on the initial data will strongly influence the orbit. This problem cannot be easily solved and might be an intrinsic limit of the Gauss algorithm. Nevertheless, this problem isn't of much importance as the eccentricity of LEO objects is always close to zero (the orbits are almost circular) and one can impose zero eccentricity for the preliminary orbit calculation, as proposed by different authors [13].

6.3 Impact of elevation

The impact of the elevation is shown in figure 8b. One can clearly observe the correlation between the correctness of the predicted heights and the position of the satellite, that is observations close to the zenith are more reliable. This problem can indeed be understood intuitively and can be solved easily by pointing the telescope to positions close to the zenith. Nevertheless, there is also a trade off as the satellites close to the zenith have a higher apparent angular velocity and are thus more difficult to capture with the telescope. The best choice might be to use angles of 60° which give good results and comparatively low satellite speeds.

6.4 Other sources of errors

It is furthermore important to notice that TLEs are always changing and must be regularly updated since they depend on the time of the observation. The reference TLEs provided are only giving the orbital elements at a given time in the past. In addition, the employed method to test the algorithms is not optimal as the provided positions of the satellites are taken from simulations. These simulations are sometimes very imprecise if the observations on which the simulations are based are older than few hours. For all those reasons it is difficult to conclude on the reliability of the algorithm.

6.5 Real image test

The test with a real image has been very difficult as the coordinates of the satellites must be extracted by hand and the satellite tracks have a considerable width as shown in figure 10. As mentioned above, already very slight differences in the input angles can completely change the orbits. In addition, the time between the different observations is rather short (one second), which is also having a negative impact on the precision. Therefore it is not surprising that the obtained results are very far from the actual orbits and that the obtained result is completely absurd (50 km height and eccentricity larger than one). Those problem will be solved by using the newly implemented image treatment algorithm the association is developing.

6.6 Improvements

As the algorithm should be able to compute precise orbits, further improvement will be needed. The following approaches could be considered in the future:

- Use range measurements with a radio-telescope or a laser in order to simplify the initial problem. In fact if the distances to the satellites are known the problem becomes a purely mathematical problem. This works fine for satellites and is already used by many institutions.
- Use a statistical approach and continuously improve the obtained orbits with more data. An idea is to observe an object one night, use the preliminary orbit determination to estimate the time of passage the next night and repeat the measurements for the same object.

The first approach is the state of the art method used in SSA, the second approach is widely used in the determination of asteroid orbits: Having a first estimate of the orbit, allows to catch the same asteroid at a later passage and to measure and improve the orbital elements [15].

6.7 Laplace and Gauss algorithm comparison

Figure 9 shows the relative errors for Gauss' and Laplace's algorithm. One can note that the two algorithms always give results close to each other and hence also errors of the same size. As the Laplace algorithm only

became functional in the last week of the project, there was not enough time to do further tests than what is shown in the report. Nevertheless, we assume that the two algorithms always give close results. This is reassuring as the two methods rely on completely different approaches, and therefore, the similarity of the results indicates that our implementations are working fine. The Laplace algorithm is very interesting as it technically allows to include more than only three observations and hence giving more accurate results. In the future it could be interesting to modify the existing Laplace algorithm in order to allow the use of more data. The two algorithms can furthermore be used to check the consistency of the obtained orbits.

7 Conclusion

The first and most important step of preliminary orbit determination is the acquisition of high quality images. Therefore, the correct handling of the mount and the calibration of the telescope are the key elements of taking qualitative measurements. Once this is mastered, it is possible to take the consecutive images needed for the the orbit interpolation. Our work has shown that very precise angle measurements are needed in order to get reliable results: even deviations in the order of arc seconds can completely change the predicted orbit. Hence, the data acquisition should be improved in order to have access to this high quality measurements. This could for example be done by increasing the exposure time (reducing the noise in the images and therefore facilitate the image treatment) and by improving the line detection algorithm. Indeed, the manual extraction of the angles is very imprecise and the fully automatized and reliable extraction of the angles is therefore indispensable. Having identified the two key parameters, elevation and time between observations, we furthermore propose the following improvements: The telescope should point at an elevation angle of about 60° and the time between the observations should ideally be larger than two seconds. As the speed of the satellites is limiting the maximal time between observations and making it impossible to attain the needed 2 s, we propose to improve the experimental setup by using a telescope mount that is able to follow the satellite and therefore take images with larger spacing in between.

The Gauss and the Laplace algorithm both allow to get a first estimate of the object's orbit, based on optical observations. The calculation of the orbital elements permit us to obtain the TLE and to compare the found data with real data. Various tests have been done with data provided by Stellarium. In general the obtained results are close to values found by institutions such as Nasa, nevertheless in some cases the predicted orbits have larger errors. Those errors appeared in the case of Gauss as well as Laplace algorithm indicating that the issue is linked to the provided input data. Indeed, different tests have shown that the elevation of the observed satellite as well as the time between observations have a critical impact on the validity of the results. Furthermore, the high precision of some of the elements, such as the inclination, strongly suggest the correct functioning of the algorithms. The systematic errors that are still found for the eccentricity for example are most possibly not due to errors in the algorithms, but rather based on imprecise measurements and could be solved by collecting more data of the same object. This is one of the suggestions for further improve the Low Orbit Satellite Tracking given by the specialists we consulted. The Laplace algorithm can be adjusted to take more observations as an input, the result will be statistically improved. Another idea might be to use a radio telescope instead of an optical telescope. This would allow a much greater accuracy of the measurements and therefore also improve the orbit prediction. A main advantage of the radio telescope is the fact that the observation gives directly the distance between the observer and the object, making it unnecessary to calculate this distance first, and therefore bypass a first source of error. Therefore, further development on the orbit interpolation has to be done in the future in order to get high accuracy orbit estimations.

References

[1] NASA Space Science Data Coordinated Archive: Sputnik 1, 27.04.2022, `https://nssdc.gsfc.nasa.gov/nmc/spacecraft/displayTrajectory.action?id=1957-001B`, last accessed: 20.05.2022.

[2] ESA - L. Boldt-Christmas: Low Earth Orbit, 02.03.2020, `https://www.esa.int/ESA_Multimedia/Images/2020/03/Low_Earth_orbit`, last accessed: 20.05.2022.

[3] ClearSpace SA: Heavy Space Traffic Ahead, 2022, https://clearspace.today, last accessed: 20.05.2022.

[4] Dr T.S. Kelso, CelesTrak: NORAD Two-Line Element Set Format, 29.12.2019, https://www.celestrak.com/NORAD/documentation/tle-fmt.php last accessed: 13.05.2022.

[5] Howard D. Curtis: Orbital Mechanics for Engineering Students, Elsevier Butterworth-Heinemann, Burlington, 2005, ISBN 0 7506 6169 0.

[6] Uotila, Urho A. and Garland, George D.: Geoid. Encyclopedia Britannica, 17 Mar. 2021, https://www.britannica.com/science/geoid, last accessed : 30.05.2022.

[7] Jet Propulsion Laboratory: Astrodynamic Parameters, California Institute of Technology, https://ssd.jpl.nasa.gov/astro_par.html, last accessed: 13.05.2022.

[8] Roger R. Bate, Donald D. Mueller, Jerry E. White: Fundamentals of Astrodynamics, Dover Publications Inc., New York, 1971, ISBN 0-486-60061-0.

[9] David A. Vallado: Fundamentals of Astrodynamics and Application, Fourth edition, The Space Technology Library, 2013.

[10] Stellatrium, satellite position data, https://stellarium-web.org/, 06.05.2022.

[11] OrbTrack, satellite position data,https://www.orbtrack.org/#/?satName=ISS%20(ZARYA), 06/05/22

[12] TLE of different satellites, https://orbit.ing-now.com, 06.05.2022.

[13] Kyle Stoker et al.: Angles-Only Orbit Determination Accuracies with Limited Observational Arc, California Polytechnic State University, 2020.

[14] R. H. Gooding, Defence Reasearch Agency, UK: A New Procedure for Orbit Determination Based on Three Lines of Sight.

[15] Alejandro Pastor, Manuel Sanjurjo-Rivo, Diego Escobar: Initial orbit determination methods for track-to-track association, Advances in Space Research, Volume 68, Issue 7, 2021.

[16] Gerhard Beutler: Methods of Celestial Mechanics I, Volume I: Physical, Mathematical, and Numerical Principles,Springer, Berlin Heidelberg, 2005, ISBN 3-540-40749-9.

[17] Werner Horn: The three anomalies, 06.06.2006, http://www.csun.edu/~hcmth017/master/node14.html, last accessed: 13.05.2022.

[18] Jeremy Tatum: Orbital elements and velocity vector, University of Victoria, 05.05.2022, https://phys.libretexts.org/Bookshelves/Astronomy__Cosmology/Celestial_Mechanics_(Tatum)/, last accessed: 13.05.2022.